Synthesis and Characterization of Palladium and Nickel Complexes with Positively Charged Triphosphine Ligands and Their Use as Electrochemical CO_2-Reduction Catalysts

Alex Miedaner, Bruce C. Noll,† and Daniel L. DuBois*

National Renewable Energy Laboratory, Golden, Colorado 80401, and the Department of Chemistry and Biochemistry, University of Colorado, Boulder, Colorado 80309

Received June 23, 1997⊗

The synthesis and characterization of $[M(Bu_3P^+etpE)Br](BF_4)_2$ (where M = Ni or Pd and $Bu_3P^+etpE = [(Bu_3PCH_2CH_2)P(CH_2CH_2PEt_2)_2]^+$) and $[M(etpPBu_3^+)Br]Br(BF_4)_4$ (where M = Ni or Pd and $etpPBu_3^+ = \{PhP[CH_2CH_2P(CH_2CH_2PBu_3)_2]_2\}^{4+}$) are described. The structure of $[Ni(etpPBu_3^+)Br]Br(BF_4)_4$ has been determined by X-ray diffraction. Treatment of $[Pd(Bu_3P^+etpE)Br](BF_4)_2$ with $AgBF_4$ in acetonitrile produced $[Pd(Bu_3P^+etpE)(CH_3CN)](BF_4)_3$. The latter compound has also been characterized by single-crystal X-ray diffraction methods. Electrochemical studies indicate that this compound and its closely related methyl analog, $[Pd(Me_3P^+etpE)(CH_3CN)](BF_4)_3$, are catalysts for the electrochemical reduction of CO_2 to CO in acidic dimethylformamide solutions. Kinetic and mechanistic studies of this catalytic reaction are reported.

Introduction

Photosynthesis is the largest renewable energy reaction occurring on Earth. In its simplest form, it can be broken down into two steps: (1) the adsorption of visible light to produce charge separation and (2) the electrochemical reduction of CO_2 to produce biomass. When coupled to photovoltaic devices or photoelectrochemical cells, the efficient electrochemical reduction of CO_2 to liquid or gaseous fuels, such as methanol or methane, would provide an alternate route to renewable fuels. This process will require major advances in both photovoltaic technology and the development of electrocatalysts for CO_2 reduction. Over the past 20 years, a number of electrocatalysts for CO_2 reduction have been developed[1−6] but many obstacles still need to be overcome before the direct electrochemical reduction of CO_2 to a fuel is feasible.

Our research on electrocatalytic reduction of CO_2 has focused on palladium complexes, such as **1** containing a tridentate phosphine ligand and a solvent molecule.[7−12] These compounds catalyze the electrochemical reduction

† University of Colorado.

⊗ Abstract published in *Advance ACS Abstracts,* December 1, 1997.

(1) For reviews of electrochemical reduction of CO_2, see: *Electrochemical and Electrocatalytic Reactions of Carbon Dioxide*; Sullivan, B. P.; Krist, K.; Guard, H. E., Eds.; Elsevier: New York, 1993. Collin, J. P.; Sauvage, J. P. *Coord. Chem. Rev.* **1989**, *93*, 245.

(2) For electrocatalysts based on transition metal complexes of nitrogen macrocycles, see: Meshitsuka, S.; Ichikawa, M.; Tamaru, K. J. *Chem. Soc., Chem Commun.* **1974**, 158. Fisher, B.; Eisenberg, R. *J. Am. Chem. Soc.* **1980**, *102*, 7363. Szalda, D. J.; Fujita, E.; Sanzenbacher, R.; Paulus, H.; Elias, H. *Inorg. Chem.* **1994**, *33*, 5855. Sakaki, S. *J. Am. Chem. Soc.* **1992**, *114*, 2055. Kelly, C. A.; Mulazzani, Q. G.; Venturi, M.; Blinn, E. L.; Rodgers, M. A. J. *J. Am. Chem. Soc.* **1995**, *117*, 4911. Smith, C. I.; Crayston, J. A.; Hay, R. W. *J. Chem. Soc., Dalton Trans.* **1993**, 3267. Pearce, D. J.; Pletcher, D. *J. Electroanal. Chem.* **1986**, *197*, 317. Schmidt, M. H.; Miskelly, G. M.; Lewis, N. S. *J. Am. Chem. Soc.* **1990**, *112*, 3420. Isse, A. A.; Gennaro, A.; Vianello, E. *J. Mol. Catal.* **1991**, *70*, 197. Fujihira, M.; Hirata, Y.; Suga, K. *J. Electroanal. Chem.* **1990**, *292*, 199. Balazs, G. B.; Anson, F. C. *J. Electroanal. Chem.* **1992**, *322*, 325. Grant, J. L.; Goswami, K.; Spreer, L. O.; Otvos, J. W.; Calvin, M. *J. Chem. Soc., Dalton Trans.* **1987**, 2105. Satake, Y.; Ihara, Y.; Senda, H.; Suzuki, M.; Uehara, A. *Inorg. Chem.* **1992**, *31*, 3248. Hammouche, M.; Lexa, D.; Momenteau, M.; Savéant, J.-M. *J. Am. Chem. Soc.* **1991**, *113*, 8455.

(3) For electrocatalysts based on transition metal complexes of bipyridine ligands, see: Hawecker, J.; Lehn, J.-M.; Ziessel, R. *Helv. Chim. Acta* **1986**, *69*, 1990. Johnson, F. P. A.; George, M. W.; Hartl, F.; Turner, J. J. *Organometallics* **1996**, *15*, 3374. Bruce, M. R. M.; Megehee, E.; Sullivan, B. P.; Thorp, H. H.; O'Toole, T. R.; Downard, A.; Pugh, J. R.; Meyer, T. J. *Inorg. Chem.* **1992**, *31*, 4864. Haukka, M.; Kiviaho, J.; Ahlgrén, M.; Pakkanen, T. A. *Organometallics* **1995**, 825. Chardon-Noblat, S.; Collomb-Dunand-Sauthier, M.-N.; Deronzier, A.; Ziessel, R.; Zsoldos, D. *Inorg. Chem.* **1994**, *33*, 4410. Christensen, P.; Hamnett, A.; Muir, V. G.; Timney, J. A.; Higgins, S. *J. Chem. Soc., Faraday Trans.* **1994**, *90*, 459. Garnier, L.; Rollin, Y.; Périchon, J. *New J. Chem.* **1989**, *13*, 53. Toyohara, K.; Tsuge, K.; Tanaka, K. *Organometallics* **1995**, *14*, 5099. Gibson, D. H.; Ding, Y.; Sleadd, B. A.; Franco, J. O.; Richardson, J. F.; Mashuta, M. S. *J. Am. Chem. Soc.* **1996**, *118*, 11984. Sende, J. A. R.; Arana, C. R.; Hernández, L.; Potts, K. T.; Keshevarz-K, M.; Abruña, H. D. *Inorg. Chem.* **1995**, *34*, 3339.

(4) For electrocatalysts based on transition metal complexes containing phosphorus ligands, see refs 7−12 and Slater, S.; Wagenknecht, J. H. *J. Am. Chem. Soc.* **1984**, *106*, 5367. Szymaszek, A.; Pruchnik, F. P. *J. Organomet. Chem.* **1989**, *376*, 133. Haines, R. J.; Wittrig, R. E.; Kubiak, C. P. *Inorg. Chem.* **1994**, *33*, 4723.

(5) For electrocatalysts based on metal electrodes, see: Shiratsuchi, R.; Nogami, G. *J. Electrochem. Soc.* **1996**, *143*, 582 and references therein. Vassiliev, Y. B.; Bagotzky, V. S.; Osetrova, N. V.; Khazova, O. A.; Mayorova, N. A. *J. Electranal. Chem.* **1985**, *189*, 271. Watanabe, M.; Shibata, M.; Kato, A.; Azuma, M.; Sakata, T. *J. Electrochem. Soc.* **1991**, *138*, 3382. Stalder, C. J.; Chao, S.; Wrighton, M. S. *J. Am. Chem. Soc.* **1984**, *106*, 3673. Eggins, B. R.; McNeill, J. *J. Electroanal. Chem.* **1983**, *148*, 17. Frese, K. W., Jr.; Leach, S. *J. Electrochem. Soc.* **1985**, *189*, 259. Hori, Y.; Kikuchi, K.; Suzuki, S. *Chem. Lett.* **1985**, 1695. Hori, Y.; Murata, A.; Tsukamoto, T.; Wakebe, H.; Koga, O.; Yamazaki, H. *Electrochim. Acta* **1994**, *39*, 2495. Jermann, B.; Augustynski, *J. Electrochim. Acta* **1994**, *39*, 1891. Cook, R. L.; MacDuff, R. C.; Sammells, A. F. *J. Electrochem. Soc.* **1990**, *137*, 187. DeWulf, D. W.; Jin, T.; Bard, A. J. *J. Electrochem. Soc.* **1989**, *136*, 1686. Naitoh, A.; Ohta, K.; Mizuno, T.; Yoshida, H.; Sakai, M.; Noda, H. *Electrochim. Acta* **1993**, *38*, 2177. Kyriacou, G.; Anagnostopoulos, A. *J. Electroanal. Chem.* **1992**, *322*, 233.

(6) For some recent reviews of different aspects of CO_2 chemistry, see: Darensbourg, D. J.; Holtcamp, M. W. *Coord. Chem. Rev.* **1996**, *153*, 155. Leitner, W. *Coord. Chem. Rev.* **1996**, *153*, 257. Costamagna, J.; Ferraudi, G.; Canales, J.; Vargas, J. *Coord. Chem. Rev.* **1996**, *148*, 221. Behr, A. *Carbon Dioxide Activation by Metal Complexes*; VCH: New York, 1988. Braunstein, P.; Matt, D.; Nobel, D. *Chem. Rev.* **1988**, *88*, 747. Some papers focusing on chemical production are as follows: Gambino, S.; Filardo, G.; Silvestri, G. *J. Appl. Electrochem.* **1982**, *12*, 549. Tsuda, T.; Maruta, K.; Kitaike, Y. *J. Am. Chem. Soc.* **1992**, *114*, 1498. Darensbourg, D. J.; Ovalles, C. *CHEMTECH* **1985**, 636. Dérien, S.; Duñach, E.; Périchon, J. *J. Am. Chem. Soc.* **1991**, *113*, 8447. Amatore, C.; Jutand, A. *J. Am. Chem. Soc.* **1991**, *113*, 2819.

S0276-7333(97)00519-0 CCC: $14.00

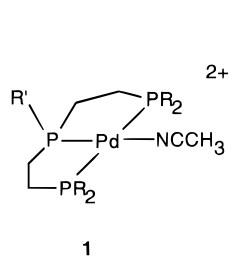

1

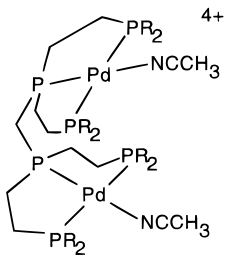

2

of CO_2 to CO. Some of these catalysts operate at relatively positive potentials and exhibit high selectivity and activity. Of special interest is the observation that the catalytic rate may be enhanced by several orders of magnitude when a second palladium atom is incorporated into catalyst **2**.[12] This rate enhancement has been attributed to cooperative binding of CO_2 by the two palladium atoms. It is thought that one palladium binds to the carbon atom of CO_2 while the second palladium atom binds to an oxygen atom.

In this paper, we describe the synthesis of nickel and palladium complexes containing tridentate ligands with pendant phosphonium groups bound to either the central or terminal phosphorus atoms. Our objective is to explore the influence of the positively charged phosphonium groups on the catalytic mechanism and rates to see if significant changes are observed. Attachment of the phosphonium groups on the periphery of the triphosphine ligand should also enhance the binding of these complexes to electrode surfaces modified with cation-exchange membranes and/or allow preparation of water-soluble complexes. These aspects will be examined in future studies.

Results

Monodentate and bidentate phosphine ligands with pendant ammonium groups have been reported for molybdenum, ruthenium, and rhodium complexes.[13] These positively charged ligands are useful for conferring water solubility on the resulting metal complexes and for immobilizing catalysts on cation-exchange resins. In principle, ligands with pendant phosphonium groups could also serve the same function and introduce a convenient ^{31}P NMR spectroscopic probe as well. The addition of PH bonds to activated olefins is a well-known reaction for the synthesis of polyphosphine ligands.[14] This reaction may proceed by either base-catalyzed or free-radical pathways. The base-catalyzed addition of PH bonds to vinylphosphonium salts has also been reported for several different phosphorus compounds.[15] We have found that extension of this reaction to triphosphine ligands results in complex reaction mixtures that are not readily purified. For example, reaction of bis((diethylphosphino)ethyl)phosphine, **3** (HetpE), with vinyltributylphosphonium bromide results in a mixture of products, eq 1. On the basis of ^{31}P

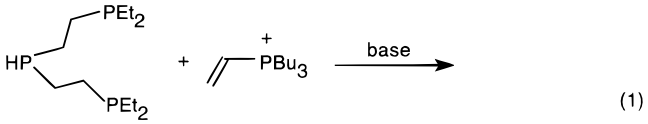

(1)

3

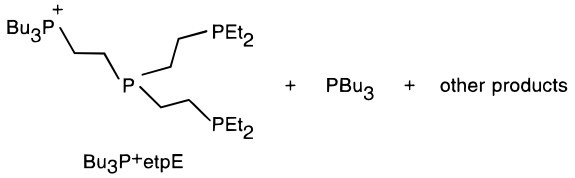

Bu_3P^+etpE

4

NMR spectra of the crude reaction mixture, approximately 50% of the product is the desired tridentate ligand **4**. Tributylphosphine, which results from a formal transfer of a vinyl cation from the vinyltributylphosphonium cation, is also formed along with numerous other products.

A more useful synthetic approach involves the coordination of the tridentate ligands **3** and **6** to palladium and nickel salts in the presence of vinyltrialkylphosphonium bromides, as shown in eqs 2 and 3. The sequence of addition of the reagents is important in these reactions. If the triphosphine ligands **3** and **6** are added to $[Pd(CH_3CN)_4](BF_4)_2$ before the phosphonium bromide, insoluble precipitates result and the reactions shown do not occur. The precipitates are presumed to result from the formation of phosphido-bridged species. If the vinyltrialkylphosphonium bromide salt is added to acetonitrile solutions of $[Pd(CH_3CN)_4](BF_4)_2$ or $[Ni(CH_3CN)_6](BF_4)_2$ first, bromide coordination occurs which prevents formation of the phosphido-bridged species. The coordinated PH groups then add cleanly to the vinyl substituent of the phosphonium cation.[16] Although the isolated yields of the phosphonium-substituted complexes in pure form are typically on the order of 50%, ^{31}P NMR studies of the reaction mixtures are consistent with greater than 90% conversion in most

(7) DuBois, D. L.; Miedaner, A. *J. Am. Chem. Soc.* **1987**, *109*, 113. DuBois, D. L.; Miedaner, A. In *Catalytic Activation of Carbon Dioxide*; ACS Symposium Series 363; American Chemical Society: Washington, DC, 1988; p 42. Steffey, B. D.; Miedaner, A.; Maciejewski-Farmer, M. L.; Bernatis, P. R.; Herring, A. M.; Allured, V.; Carperos, V.; DuBois, D. L. *Organometallics* **1994**, *13*, 4844. Herring, A. M.; Steffey, B. D.; Miedaner, A.; Wander, S. A.; DuBois, D. L. *Inorg. Chem.* **1995**, *34*, 1100.

(8) Miedaner, A.; Curtis, C. J.; Barkley, R. M.; DuBois, D. L. *Inorg. Chem.* **1994**, *33*, 5482.

(9) DuBois, D. L.; Miedaner, A.; Haltiwanger, R. C. *J. Am. Chem. Soc.* **1991**, *113*, 8753.

(10) Bernatis, P. R.; Miedaner, A.; Haltiwanger, R. C.; DuBois, D. L. *Organometallics* **1994**, *13*, 4835.

(11) Wander, S. A.; Miedaner, A.; Noll, B. C.; DuBois, D. L. *Organometallics* **1996**, *15*, 3360.

(12) Steffey, B. D.; Curtis, C. J.; DuBois, D. L. *Organometallics* **1995**, *14*, 4937.

(13) Töth, I.; Hanson, B. E.; Davis, M. E. *J. Organomet. Chem.* **1990**, *397*, 109. Smith, R. T.; Ungar, R. K.; Sanderson, L. J.; Baird, M. C. *Organometallics* **1983**, *2*, 1138. Renaud, E.; Baird, M. C. *J. Chem. Soc., Dalton Trans.* **1992**, 2905. Renaud, E.; Baird, M. C. *J. Mol. Catal.* **1993**, *80*, 43. Smith, R. T.; Baird, M. C. *Inorg. Chim. Acta* **1982**, *62*, 135. Renaud, E.; Russell, R. B.; Fortier, S.; Brown, S. J.; Baird, M. C. *J. Organomet. Chem.* **1991**, *419*, 403. Mohr, B.; Lynn, D. M.; Grubbs, R. H. *Organometallics* **1996**, *15*, 4317.

(14) King, R. B. In *Catalytic Aspects of Metal Phosphine Complexes*; Alyea, E. C., Meek, D. W., Eds.; Advances in Chemistry Series 196; American Chemical Society: Washington, DC, 1982; p 313. DuBois, D. L.; Myers, W. H.; Meek, D. W. *J. Chem. Soc., Dalton Trans.* **1975**, 1011.

(15) Keough, P. T.; Grayson, M. *J. Org. Chem.* **1964**, *29*, 631. Grayson, M.; Keough, P. T. U.S. Patent 3 689 601, 1972.

(16) There are a number of precedents for the addition of coordinated primary and secondary phosphines to olefins, see: Brauer, D. J.; Lebbe, T.; Stelzer, O. *Angew. Chem.* **1988**, *100*, 432. Diel, B. N.; Haltiwanger, R. C.; Norman, A. D. *J. Am. Chem. Soc.* **1982**, *104*, 4700. Leoni, P.; Pasquali, M.; Sommovigo, M.; Albinati, A.; Lianza, F.; Pregosin, P. S.; Rüegger, H. *Organometallics* **1993**, *12*, 4503.

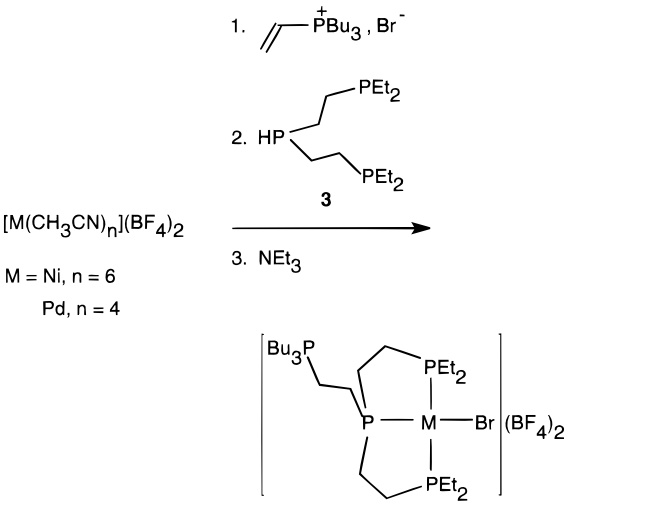

5a M = Pd
5b M = Ni (2)

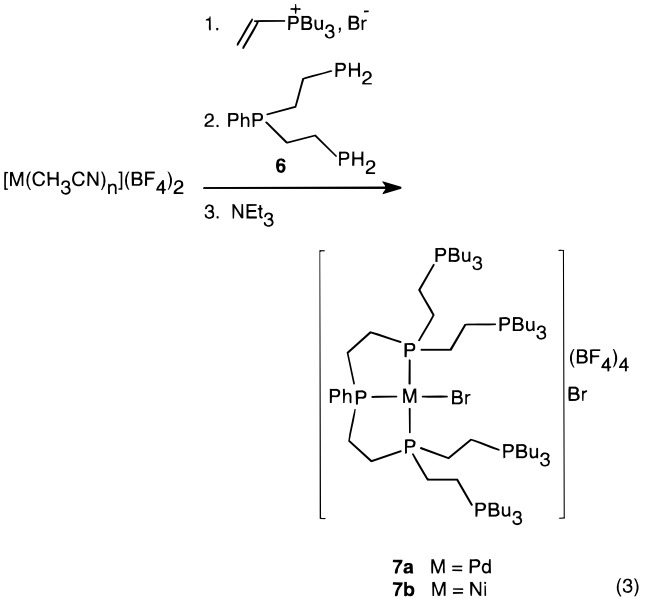

7a M = Pd
7b M = Ni (3)

cases. Complexes [Pd(etpPBu$_3^+$)Br]Br(BF$_4$)$_4$ (**7a**) and [Ni(etpPBu$_3^+$)Br]Br(BF$_4$)$_4$ (**7b**), which contain four phosphonium substituents attached to the terminal phosphorus atoms of the triphosphine ligand, are more difficult to obtain in pure form than [Pd(Bu$_3$P$^+$etpE)Br](BF$_4$)$_2$ (**5a**) and [Ni(Bu$_3$P$^+$etpE)Br](BF$_4$)$_2$ (**5b**).

Complexes **5a,b** and **7a,b** are air stable in the solid state and in solution. These complexes have been characterized by elemental analysis, ^{1}H and ^{31}P NMR spectroscopy, and cyclic voltammetry. The structure of **7b** has been confirmed by an X-ray diffraction study. The ^{1}H NMR spectra, listed in the Supporting Information, are consistent with the proposed structures but are complicated by the presence of multiple overlapping resonances and additional P−H coupling. The ^{31}P NMR data are more diagnostic and are given in Table 1. For complexes **5a** and **5b,** the resonance for the phosphonium group is a doublet at approximately 37 ppm. The observed coupling between the phosphonium substituent and the central phosphorus atom of the tridentate ligand is similar to other three-bond P−P coupling constants and confirms the addition of the P−H bond to the vinylphosphonium salt.[17] The resonances assigned to the central phosphorus atoms of **5a** and **5b** are doublets of triplets due to coupling of the central phosphorus atom to the phosphonium group and the terminal phosphorus atoms of the tridentate ligand. The chemical shifts of these resonances and the magnitude of the coupling between the central and terminal phosphorus atoms are similar to those observed in other Pd and Ni triphosphine complexes.[17] The doublets expected for the terminal phosphorus atoms occur at approximately 60 ppm.

Both [Pd(etpPBu$_3^+$)Br]Br(BF$_4$)$_4$ (**7a**) and [Ni(etpPBu$_3^+$)Br]Br(BF$_4$)$_4$ (**7b**) exhibit second-order ^{31}P NMR spectra, as shown in Figure 1 for **7b** (upward trace). This spectrum has been analyzed as an AA′BB′MM′X spin system, and the simulated spectrum is shown in Figure 1 as the downward trace.[18] Four major resonances are observed. Two of them, centered at 37.70 and 37.37 ppm, are assigned to the pendant phosphonium groups. The phenyl group on the central phosphorus is directed above the plane defined by palladium and its four ligands, as shown in structure **1**, and as a result, the two phosphonium substituents on the same side of the plane as the phenyl group have slightly different chemical shifts from the two phosphonium substituents on the side opposite the phenyl group. The complex resonance for the terminal phosphorus atoms of the triphosphine ligand occurs at 55.34 ppm, which is similar to the chemical shifts observed for terminal phosphorus atoms of [Pd(Bu$_3$P$^+$etpE)Br](BF$_4$)$_2$ (**5a**) and [Ni(Bu$_3$P$^+$etpE)Br](BF$_4$)$_2$ (**5b**). The resonance for the central phosphorus atom is a simple triplet at 116.16 ppm. The good agreement between the experimental and simulated spectra and the values observed for the chemical shifts and coupling constants provide unambiguous evidence that all four phosphonium groups are bound to the terminal phosphorus atom of the triphosphine ligand via an ethylene bridge.

The acetonitrile complexes [Pd(Bu$_3$P$^+$etpE)(CH$_3$CN)](BF$_4$)$_3$ (**8a**), [Ni(Bu$_3$P$^+$etpE)(CH$_3$CN)](BF$_4$)$_3$ (**8b**), [Pd(Me$_3$P$^+$etpE)(CH$_3$CN)](BF$_4$)$_3$ (**8c**), and [Pd(etpPBu$_3^+$)(CH$_3$CN)](BF$_4$)$_6$ (**9**) can be prepared from their corresponding bromide complexes by treatment with AgBF$_4$ in acetonitrile. With the exception of **9**, these complexes can be obtained as crystalline, analytically pure compounds. We were unable to achieve a complete separation of **9** and the vinyltributylphosphonium salt used to prepare it. The ^{31}P NMR spectra of the acetonitrile complexes are similar to their bromide analogs, and the spectral data for these compounds are presented in Table 1. The presence of coordinated acetonitrile in these complexes is confirmed by the observation of two infrared bands at approximately 2300 and 2325 cm^{-1} that are assigned to CN stretching and combination modes.[19] The acetonitrile ligands in these complexes are labile and can be easily displaced. For example, reaction of **8a** with triethylphosphine results in the formation of [Pd(Bu$_3$P$^+$etpE)(PEt$_3$)](BF$_4$)$_3$, **10**.

Structural Studies. Confirmation of the structure of [Ni(etpPBu$_3^+$)Br](BF$_4$)$_4$Br (**7b**) was provided by an X-ray diffraction study. Single crystals of **7b** were grown from a mixture of dichloromethane and ethyl acetate by slow evaporation of the solvent. The orange

(17) Garrou, P. E. *Chem. Rev.* **1981**, *81*, 229.
(18) Spectral simulations were carried out using *gNMR*, version 3, by Cherwell Scientific Publishing Ltd.
(19) Storhoff, B. N.; Lewis, H. C. *Coord. Chem. Rev.* **1977**, *23*, 1.

Table 1. $^{31}P\{^{1}H\}$ NMR Data for Metal Complexes

	δ (ppm)[a]			J (Hz)			
compound	P_C[b]	P_T	P^+	J_{CT}	J_{CP^+}	J_{TP^+}	$J_{TT'}$
$[Pd(Bu_3P^+etpE)Br]^{2+}$	116.8 (dt)	59.6 (d)	37.2 (d)	6	41		
$[Ni(Bu_3P^+etpE)Br]^{2+}$	118.2 (dt)	60.9 (d)	37.0 (d)	44	36		
$[Pd(Bu_3P^+etpE)NCCH_3]^{3+}$	118.1 (dt)	64.2 (d)	37.5 (d)	6	44		
$[Ni(Bu_3P^+etpE)NCCH_3]^{3+}$	114.3 (dt)	63.1 (d)	37.3 (d)	46	40		
$[Pd(Me_3P^+etpE)NCCH_3]^{3+}$	117.9 (dt)	64.5 (d)	32.4 (d)	6	51		
$[Pd(Bu_3P^+etpE)PEt_3]^{3+}$	118.9 (ddt)	57.2 (dd)	37.5 (dd)	12	35		
			11.8 (PEt_3, ddt)[c]			32 (J_{TL})[c]	310 (J_{CL})[c]
$[Pd(etpPBu_3^+)Br]^{5+}$	117.67 (t)	57.88 (m)	37.55 (t)	6		46	~450
			37.64 (t)			52	
$[Ni(etpPBu_3^+)Br]^{5+}$	116.16 (t)	55.34 (m)	37.37 (t)	44		45.2, 41.5	~350
			37.70 (t)				
$[Pd(etpPBu_3^+)NCCH_3]^{6+}$	120.6 (t)	61.8 (m)	37.43 (t)	7		44	~450
			37.60 (t)			42	

[a] All spectra were recorded at 121.1 MHz (300 MHz for proton) in either acetonitrile-d_3 or acetone-d_6 solutions. The chemical shifts are given in ppm relative to external phosphoric acid. [b] Central, terminal, and phosphonium phosphorus atoms are designated by the subscripts C and T and the superscript $^+$, respectively. [c] Resonance and coupling arising from triethylphosphine.

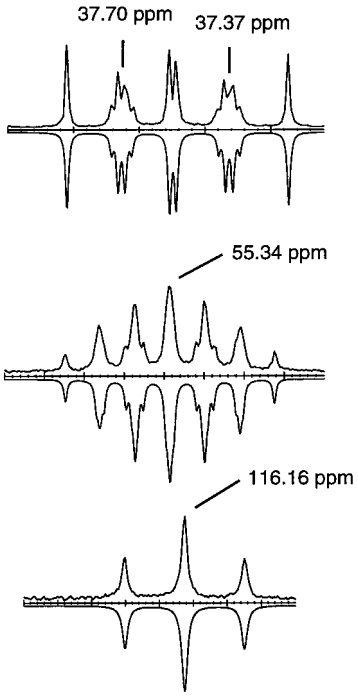

Figure 1. ^{31}P NMR spectrum of $[Ni(etpPBu_3^+)Br]Br(BF_4)_4$ (**7b**) in acetonitrile-d_3. The upward trace is the experimental spectrum, and the downward trace is the spectrum calculated using the parameters listed in Table 1. Each division is 10 Hz in the top spectral region, and each division is 20 Hz in the middle and bottom spectral regions.

crystals consist of the cation of **7b**, four tetrafluoroborate anions, a bromide ion, a disordered dichloromethane molecule, and a disordered ethyl acetate molecule. A drawing of the cation of **7b** is shown in Figure 2, and important bond lengths and angles are given in Table 2. The coordination geometry about nickel is that of a distorted square plane with three phosphorus atoms and a bromide ion occupying the coordination sites. The sum of the four angles formed by the donor atoms to nickel is 360.2°, which indicates nearly planar coordination. The bond angles between the terminal and central phosphorus atoms of the triphosphine ligand [P(4)−Ni−P(5) and P(4)−Ni−P(1)] are approximately 85°, as expected for a five-membered chelate ring. The Br(1)-Ni-P(1) and Br(1)−Ni−P(5) bond angles are 99.3° and 90.9°, respectively, and this nonequivalence suggests a steric interaction between one of the pendant tributylphos-phonium substituents and the bromide ligand.

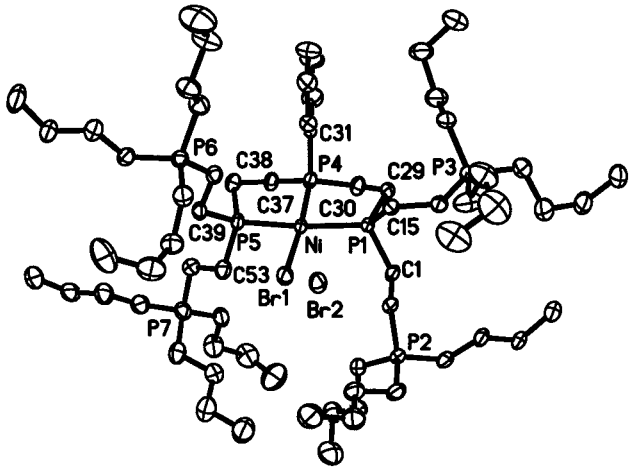

Figure 2. Perspective drawing of the $[Ni(etpPBu_3^+)Br]^{5+}$ (**7b**$^{5+}$) cation and the bromide counterion with 50% thermal ellipsoids shown.

Table 2. Selected Bond Lengths (Å) and Angles (deg) for $[Ni(etpPBu_3^+)Br](BF_4)_4Br$, 7b

Ni−P(4)	2.128(2)	Ni−P(5)	2.201(2)
Ni−P(1)	2.2140(15)	Ni−Br(1)	2.3325(9)
P(1)−C(15)	1.833(6)	P(1)−C(1)	1.848(5)
P(1)−C(29)	1.852(6)	P(2)−C(2)	1.800(5)
P(2)−C(3)	1.801(6)	P(2)−C(7)	1.805(6)
P(2)−C(11)	1.816(6)	P(4)−C(31)	1.815(6)
P(4)−C(37)	1.818(6)	P(4)−C(30)	1.827(6)
P(5)−C(39)	1.836(5)	P(5)−C(38)	1.841(6)
P(5)−C(53)	1.853(6)		

P(4)−Ni−P(5)	85.36(6)	P(4)−Ni−P(1)	84.60(6)
P(5)−Ni−P(1)	169.50(6)	P(4)−Ni−Br(1)	174.45(5)
P(5)−Ni−Br(1)	90.94(5)	P(1)−Ni−Br(1)	99.29(5)
C(15)−P(1)−C(1)	105.5(3)	C(15)−P(1)−C(29)	104.8(3)
C(1)−P(1)−C(29)	103.1(3)	C(15)−P(1)−Ni	117.4(2)
C(1)−P(1)−Ni	114.9(2)	C(29)−P(1)−Ni	109.7(2)
C(2)−P(2)−C(3)	108.0(3)	C(2)−P(2)−C(7)	107.3(3)
C(3)−P(2)−C(7)	110.6(3)	C(2)−P(2)−C(11)	110.7(3)
C(3)−P(2)−C(11)	108.7(3)	C(7)−P(2)−C(11)	111.4(3)
C(31)−P(4)−C(37)	106.6(3)	C(31)−P(4)−C(30)	105.8(3)
C(37)−P(4)−C(30)	112.1(3)	C(31)−P(4)−Ni	112.4(2)
C(37)−P(4)−Ni	109.7(2)	C(30)−P(4)−Ni	110.3(2)
C(39)−P(5)−C(38)	106.6(3)	C(39)−P(5)−C(53)	106.3(3)
C(38)−P(5)−C(53)	108.6(3)	C(39)−P(5)−Ni	117.2(2)
C(38)−P(5)−Ni	109.6(2)	C(53)−P(5)−Ni	108.2(2)

The Ni−P(4) bond length is 0.07−0.09 Å shorter than the Ni−P(5) and Ni−P(1) bond lengths. Other structurally characterized complexes containing triphosphine ligands show a similar shortening of the bond between the central phosphorus atom and the metal.[20] This

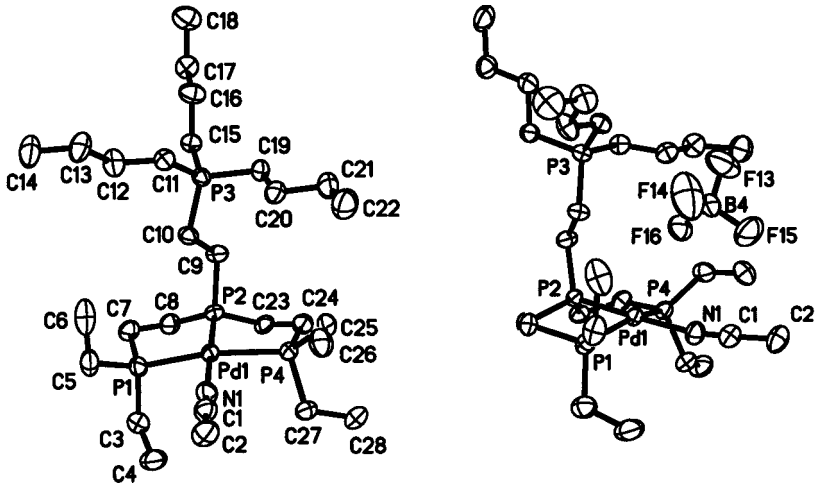

Figure 3. Perspective drawings of the $[Pd(Bu_3P^+etpE)(CH_3CN)]^{3+}$ (**8a**$^{3+}$) cation and one tetrafluoroborate counterion with 50% thermal ellipsoids shown.

difference may reflect a difference in the vibrational amplitude of the central phosphorus atom because of its incorporation in two five-membered rings and/or a greater trans influence for P compared to Br^-. The structure clearly supports the addition of all four P−H bonds to form the quadruply charged triphosphine ligand. During the crystallization process, the BF_4^- anions crystallize in preference to the bromide ion, which results in four fluoroborate ions on the periphery of the cation. The bromide ion that is not bound to Ni resides in a pocket formed by two pendant phosphonium groups above the Ni atom on the face opposite the phenyl substituent, as shown in Figure 2. The Ni−Br distance of 3.52 Å is nonbonding, consistent with the planarity of Ni and the atoms of the inner coordination sphere.

Single crystals of $[Pd(Bu_3P^+etpE)(CH_3CN)](BF_4)_3$ (**8a**) were grown from a solution of ethyl acetate and dichloromethane containing approximately 5% acetonitrile. The crystals are composed of the two independent $[Pd(Bu_3P^+etpE)(CH_3CN)]^{3+}$ cations and BF_4^- anions. A drawing of one cation and an associated BF_4^- anion is shown in Figure 3, and important bond lengths and angles are given in Table 3. The structure of the palladium cation is a distorted square plane with three coordination sites occupied by the triphosphine ligand and the fourth by acetonitrile. The sum of the four angles formed by the donor atoms to palladium is 360.4°, consistent with nearly planar coordination. The conformation of the five-membered rings formed by Pd and the triphosphine ligand are all in the envelope form with the carbons adjacent to the central phosphorus atom forming the apex of the tab. The tributylphosphonium group is clearly attached to the central phosphorus atom via an ethylene linkage, and a BF_4^- anion is positioned so that it appears to be interacting with both the palladium atom and the phosphonium group. The Pd(1)−F(16) and P(3)−F(16) distances are 3.21 and 4.04 Å, respectively. From computer models, it is clear that the BF_4^- anion is in van der Waals contact with both the palladium atom and methylene substituents adjacent to the phosphonium phosphorus.

Table 3. Selected Bond Lengths (Å) and Angles (deg) for $[Pd(Bu_3P^+etpE)(CH_3CN)](BF_4)_3$, 8a

Pd(1)−N(1)	2.080(4)	Pd(1)−P(2)	2.2126(10)
Pd(1)−P(1)	2.3173(13)	Pd(1)−P(4)	2.3239(14)
N(1)−C(1)	1.121(6)	P(1)−C(5)	1.792(6)
P(1)−C(7)	1.828(5)	P(1)−C(3)	1.857(5)
P(2)−C(8)	1.817(5)	P(2)−C(23)	1.818(5)
P(2)−C(9)	1.829(4)	P(3)−C(11)	1.796(5)
P(3)−C(19)	1.805(5)	P(3)−C(15)	1.807(4)
P(3)−C(10)	1.814(4)	P(4)−C(25)	1.813(5)
P(4)−C(27)	1.825(5)	P(4)−C(24)	1.842(5)
N(1)−Pd(1)−P(2)	178.29(11)	N(1)−Pd(1)−P(1)	96.62(13)
P(2)−Pd(1)−P(1)	84.57(5)	N(1)−Pd(1)−P(4)	95.26(14)
P(2)−Pd(1)−P(4)	83.99(4)	P(1)−Pd(1)−P(4)	158.25(5)
C(1)−N(1)−Pd(1)	170.8(4)	C(5)−P(1)−C(7)	107.3(3)
C(5)−P(1)−C(3)	107.6(3)	C(7)−P(1)−C(3)	104.6(2)
C(5)−P(1)−Pd(1)	121.4(2)	C(7)−P(1)−Pd(1)	108.2(2)
C(3)−P(1)−Pd(1)	106.6(2)	C(8)−P(2)−C(23)	110.0(2)
C(8)−P(2)−C(9)	109.3(2)	C(23)−P(2)−C(9)	104.4(2)
C(8)−P(2)−Pd(1)	111.0(2)	C(23)−P(2)−Pd(1)	109.3(2)
C(9)−P(2)−Pd(1)	112.62(15)	C(11)−P(3)−C(19)	109.6(2)
C(11)−P(3)−C(15)	110.6(2)	C(19)−P(3)−C(15)	108.6(2)
C(11)−P(3)−C(10)	106.8(2)	C(19)−P(3)−C(10)	110.8(2)
C(15)−P(3)−C(10)	110.5(2)	C(25)−P(4)−C(27)	106.5(3)
C(25)−P(4)−C(24)	105.3(2)	C(27)−P(4)−C(24)	107.6(3)
C(25)−P(4)−Pd(1)	122.6(2)	C(27)−P(4)−Pd(1)	105.4(2)
C(24)−P(4)−Pd(1)	108.7(2)	N(1)−C(1)−C(2)	178.2(6)

Electrochemical Studies. The electrochemical data for the complexes prepared in this work are summarized in Table 4. The data for selected complexes are discussed in more detail to emphasize the role of the monodentate ligand in determining the electrochemical behavior of individual complexes. Cyclic voltammograms of $[Pd(Bu_3P^+etpE)(Br)](BF_4)_2$ (**5a**) and $[Pd(Bu_3P^+etpE)(PEt_3)](BF_4)_3$ (**10**) are shown in Figure 4. For the triethylphosphine complex, a nearly reversible reduction wave is observed at −1.33 V vs the ferrocene/ferrocenium couple. Plots of the peak current vs the square root of the scan rate ($\nu^{1/2}$) are linear, which implies a diffusion-controlled process.[21] A peak-to-peak separation of 47 mV for a scan rate of 20 mV/s is consistent with a two-electron reduction that is slightly broadened from the expected 30 mV by slow electron transfer.[21] The ratio of the anodic peak current to the cathodic peak current is 0.9, and controlled-potential electrolysis at −1.45 V resulted in the passage of 1.8 *F*/mol of complex.

(20) Saum, S. E.; Laneman, S. A.; Stanley, G. G. *Inorg. Chem.* **1990**, *29*, 5065. Jia, G.; Lee, H. M.; Williams, I. D. *Organometallics* **1996**, *15*, 4235.

(21) Bard, A. J.; Faulkner, L. R. *Electrochemical Methods*; Wiley: New York, 1980; pp 218−231, 453, 200−204.

Table 4. Electrochemical Data for Complexes in Dimethylformamide Solutions

compound	$E_{1/2}$[a] II/I, II/0[e]	$E_{1/2}$[a] I/0	ΔE_p[b]	i_{pa}/i_{pc}[c]	n[d]
$[Pd(Bu_3P^+etpE)Br]^{2+}$	−1.73 (i)[e] [−1.27, −1.16]		(64)	0	1.9
$[Ni(Bu_3P^+etpE)Br]^{2+}$	−1.41 (r)	−1.87 (i) [−1.2]	76, (63)	1.0	1.2
$[Pd(Bu_3P^+etpE)NCCH_3]^{3+}$	−1.52 (i)[f]		(150)	0	1.0[g]
$[Ni(Bu_3P^+etpE)NCCH_3]^{3+}$	−1.31 (i)	−1.57 (i)		0	1.0
$[Pd(Bu_3P^+etpE)PEt_3]^{3+}$	−1.33 (r)[e]		51	0.87	1.8
$Pd(Me_3P^+etpE)NCCH_3]^{3+}$	−1.45 (q)[f]		185	0.48	1.0[g]
$[Pd(etpPBu_3^+)Br]^{5+}$	−1.50 (q)[e]		115	0.69	2.0
$[Ni(etpPBu_3^+)Br]^{5+}$	−1.38 (q)	−1.62 (q)	307, 80	0.34	1.0
$[Pd(etpPBu_3^+)NCCH_3]^{6+}$	−1.4 (i)[h]				

[a] Half-wave potentials for reversible couples and peak potentials for irreversible couples. All values are with respect to the ferrocene/ferrocenium couple. Labels in parentheses indicate whether the wave is reversible (r), quasi-reversible (q), or irreversible (i). Numbers in brackets indicate the peaks of associated oxidation waves. For nickel complexes, there are typically two well-resolved reduction waves. For palladium complexes under nitrogen atmospheres, only one reduction wave is observed. [b] Difference between associated cathodic and anodic peaks for reversible or quasi-reversible waves. Values shown in parentheses are the difference between the peak-cathodic current and the half-wave current for waves that do not exhibit an associated anodic wave. [c] Ratio of peak-anodic to peak-cathodic current for the first reduction wave. [d] Number of Faradays of charge passed per mole of complex at potentials approximately 100 mV negative of the first reduction wave listed for each complex. [e] These waves correspond to a two-electron reduction from Pd(II) to Pd(0). [f] Half-wave potentials for these complexes were calculated from the peak potentials in the presence of CO_2 using eq 11.3.23 of ref 21 and the rate constants given in the text. [g] Reduction carried out in the presence of CO_2. [h] Onset of a broad, poorly defined reduction wave.

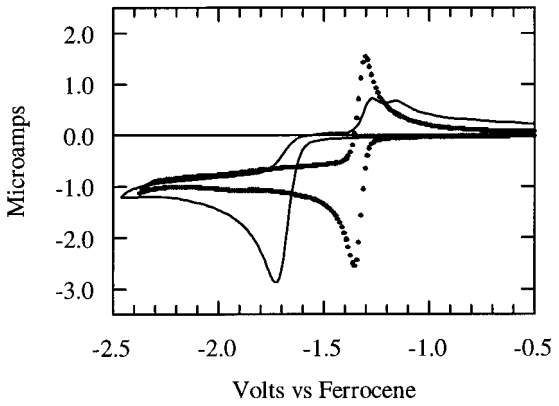

Figure 4. Cyclic voltammograms of 0.0016 M $[Pd(Bu_3P^+etpE)(PEt_3)](BF_4)_3$ (**10**) (···) and 0.0019 M $[Pd(Bu_3P^+etpE)Br](BF_4)_2$ (**5a**) (−) in 0.3 M NEt_4BF_4 in dimethylformamide. The working electrode was glassy carbon, and the scan rate was 0.05 V/s. Potentials are given vs the ferrocene/ferrocenium couple.

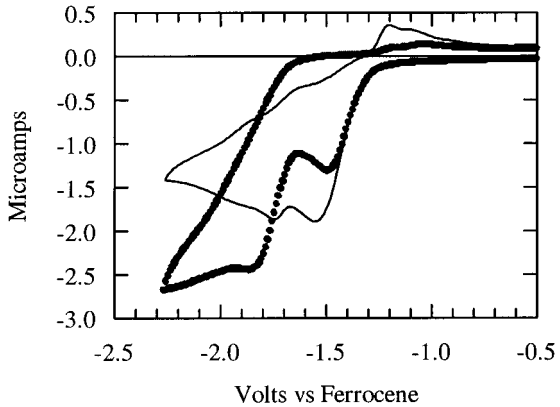

Figure 5. Cyclic voltammograms of 0.0024 M $[Pd(Bu_3P^+etpE)(CH_3CN)](BF_4)_3$ (**8a**) in the presence of 0.18 M CO_2 (solid circles) and under a nitrogen atmosphere (solid line). Other conditions were the same as those given in Figure 4.

All of these data are consistent with a simple, quasi-reversible, two-electron reduction.

For the bromide complex, $[Pd(Bu_3P^+etpE)Br](BF_4)_2$ (**5a**), an irreversible reduction wave is observed at −1.73 V vs the ferrocene/ferrocenium couple. Associated with this wave are two anodic waves with peaks at −1.27 and −1.16 V. The cathodic wave is diffusion controlled, as indicated by a linear plot of the peak current vs $\nu^{1/2}$. A controlled-potential electrolysis carried out at −1.9 V resulted in the passage of 1.9 *F*/mol of complex, consistent with a two-electron process. The difference between the peak potential and the half-wave potential is 62 mV at a scan rate of 50 mV/s. The shift of the peak potential is approximately 30 mV per decade change in the scan rate. These data are consistent with a quasi-reversible two-electron reduction of **5a** followed by a fast irreversible chemical reaction.[21] Most likely, the irreversible reaction is loss of halide from the Pd(0) complex generated on reduction.

Replacing the bromide ligand with acetonitrile results in a shift of the reduction potential in a positive direction to −1.55 V for $[Pd(Bu_3P^+etpE)(CH_3CN)](BF_4)_3$ (**8a**). In this case, the reduction wave is broader and less well-defined, as shown by the solid line of Figure 5. When the potential is reversed immediately after traversing the reduction wave at −1.55 V, the oxidation wave at −1.20 V is still observed. Controlled-potential electrolysis of this complex under nitrogen at -1.9 V resulted in the passage of 1.9 *F*/mol of complex. A chronoamperometric experiment in which the potential was stepped from −1.2 to −1.9 V resulted in a slope that was consistent with the passage of 2.0 *F*/mol when normalized to 2.0 electrons for the triethylphosphine complex, $[Pd(Bu_3P^+etpE)(PEt_3)](BF_4)_3$ (**10**). These data are most consistent with complex **8a** undergoing two closely spaced one-electron reductions that are followed by an irreversible chemical reaction.

In the presence of CO_2, the first reduction wave of $[Pd(Bu_3P^+etpE)(CH_3CN)](BF_4)_3$ decreases in height to 65% of the value observed under nitrogen and shifts in a positive direction by 75 mV, as shown in Figure 5 (solid circles). In addition, a second wave is observed at −1.87 V. The decreased height of the first wave is consistent with a one-electron reduction, as shown in the first step of eq 4. A one-electron reduction is also supported by chronoamperometric experiments. In these experiments, the potential was stepped from a value positive of the first reduction wave to a potential negative of this wave under both CO_2 and N_2 atmospheres. For complex **8a**, the slope of a plot of charge vs the square root of time ($t^{1/2}$) in the presence of CO_2

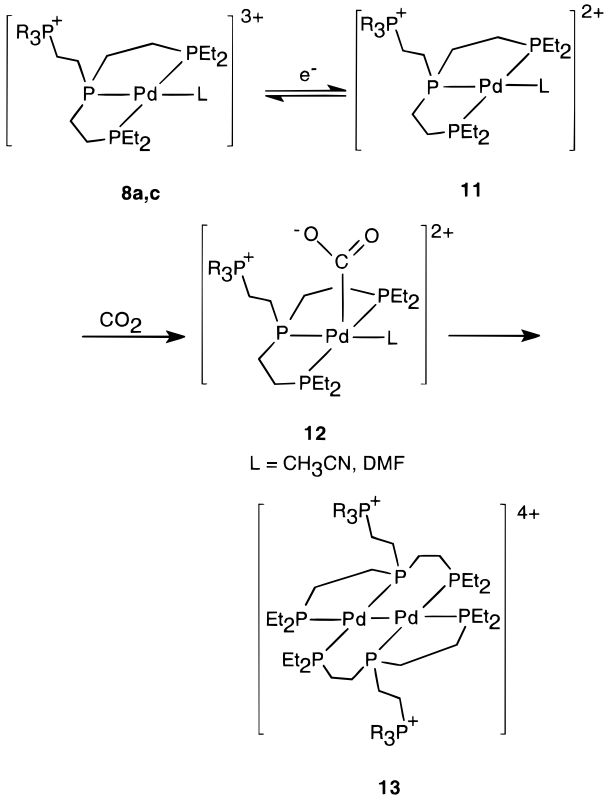

is half that of the slope in the presence of nitrogen. As discussed above, **8a** undergoes a two-electron reduction under nitrogen. Because the slope of the plot of the charge passed as a function of $t^{1/2}$ is proportional to the number of electrons involved in the reduction process,[21] the decreased slope implies a one-electron reduction of **8a** occurs in the presence of CO_2. The controlled-potential electrolysis experiments discussed below are also consistent with a one-electron reduction of **8a** in the presence of CO_2. Finally, recent electrochemical studies of palladium complexes containing triarsine ligands are consistent with two sequential one-electron reductions with detectable Pd(I) intermediates.[22]

Step 2 of eq 4, the reaction of CO_2 with the Pd(I) intermediate generated upon reduction, is supported by three observations. First, the shift of the peak potential in a positive direction in the presence of CO_2 is characteristic of a reversible electron transfer followed by a fast irreversible reaction with CO_2. Second, the decrease in the peak height is also indicative of a reaction with CO_2 following reduction. Third, as discussed below in the section on catalytic studies, the catalytic current shows a square root dependence on the CO_2 concentration. This result is consistent with a rate-determining step that is first order in CO_2. All of these observations support the reaction of a Pd(I) intermediate such as **11** with CO_2.

In eq 4, complex **11** is shown as a four-coordinate species. Because the electron acquired in the first step would be expected to reside in a molecular orbital that is antibonding with respect to the solvent molecule, an irreversible loss of solvent might be expected to precede the reaction with CO_2. However, if a fast irreversible loss of solvent occurred after reduction of **8a** but prior to CO_2 binding, the rate of solvent loss should determine

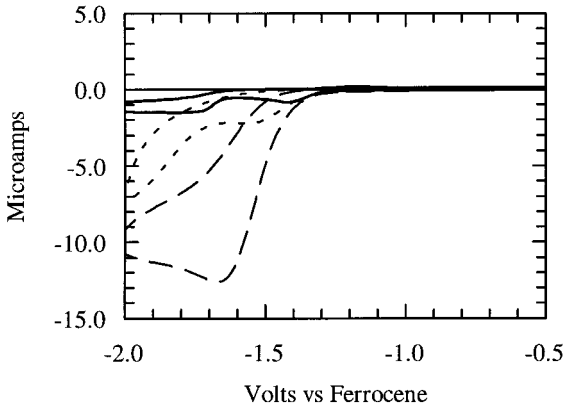

Figure 6. Cyclic voltammograms of 0.0013 M [Pd(Me_3P^+etpE)(CH_3CN)](BF_4)$_3$ (**8c**) in the presence of 0.18 M CO_2 (−), 0.023 M HBF_4 under nitrogen (···), and 0.023 M HBF_4 and 0.18 M CO_2 (- - -). Other conditions were the same as those given in Figure 4.

the peak potential and CO_2 should have no effect. Because CO_2 does shift the potential, it is concluded that the Pd(I) species reacting with CO_2 is four-coordinate, as shown in eq 4. The transition state which results from interaction of this four-coordinate intermediate, **11**, with CO_2 would then be five-coordinate, as shown for **12.** Isoelectronic, five-coordinate Ni(I)CO_2 complexes have also been detected as intermediates by other researchers.[23]

Controlled-potential electrolysis of **8a** under CO_2 at −1.6 V resulted in the passage of 1.0 *F*/mol of complex. In comparison, the reduction of **8a** under nitrogen resulted in passage of 1.9 *F*/mol of complex, as discussed above. Clearly, CO_2 plays an important role in the reduction process observed for this complex. The product formed by the reduction of **8a** under CO_2 was characterized by ^{31}P NMR spectroscopy and cyclic voltammetry and assigned a dimeric structure with bridging triphosphine ligands. Both the NMR data and electrochemical data are similar to those of [Pd(etpE)]$_2$(BF_4)$_2$, which has been characterized as a Pd(I) dimer by an X-ray diffraction study (see Experimental Section).[9] In summary, in the presence of CO_2, **8a** undergoes a one-electron reduction to form a transient Pd(I)CO_2 complex, which undergoes decomposition to a Pd(I) dimer, **13**, with bridging triphosphine ligands (eq 4). In the absence of CO_2, a two-electron reduction is observed for **8a**.

Catalytic Studies. Cyclic voltammograms of [Pd(Me_3P^+etpE)(CH_3CN)](BF_4)$_3$ (**8c**) in the presence of both HBF_4 and CO_2 (dashed line), in the presence of HBF_4 but no CO_2 (dotted line), and under CO_2 but no acid (solid line) are shown in Figure 6. From these results, it is clear that both acid and CO_2 are required for catalysis. Controlled-potential electrolysis of **8c** in a DMF solution saturated with CO_2 and containing 0.03 M HBF_4 was carried out at −1.65 V. A current efficiency of 45% for CO production was observed, with hydrogen production accounting for the remaining current. A turnover number of 15 based on CO was obtained.

Similar electrochemical studies were carried out for the other compounds shown in Table 4. Of these

(22) Downard, A. J.; Bond, A. M.; Clayton, A. J.; Hanton, L. R.; McMorrau, D. A. *Inorg. Chem.* **1996**, *35*, 7684.

(23) Fujita, E.; Haff, J.; Sanzenbacher, R.; Elias H. *Inorg. Chem.* **1994**, *33*, 4627.

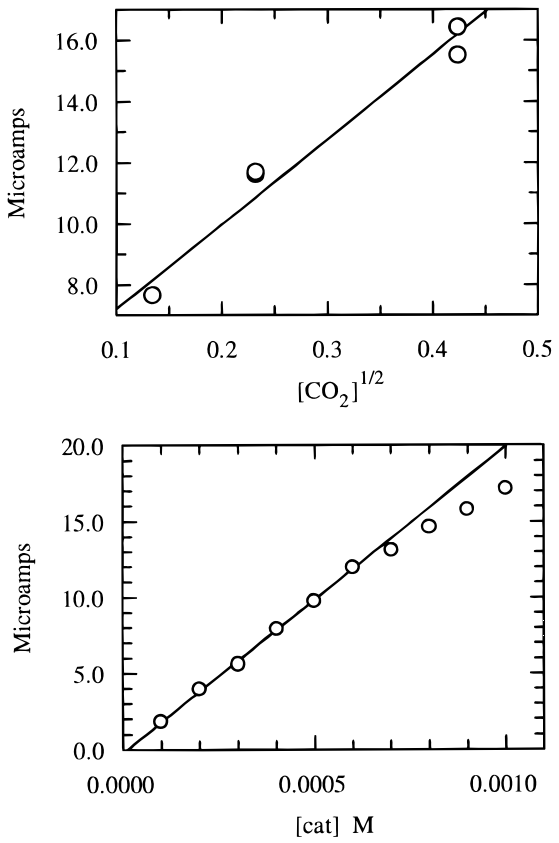

Figure 7. Dependence of the peak current on the concentration of CO_2 for dimethylformamide solutions containing 0.0013 M $[Pd(Me_3P^+etpE)(CH_3CN)](BF_4)_3$ (**8c**) and 0.038 M HBF_4 (top graph). Dependence of the peak current on the concentration of $[Pd(Me_3P^+etpE)(CH_3CN)](BF_4)_3$ for dimethylformamide solutions containing 0.18 M CO_2 and 0.038 M HBF_4 (bottom graph).

compounds, only $[Pd(Bu_3P^+etpE)(CH_3CN)](BF_4)_3$ (**8a**) and $[Pd(Me_3P^+etpE)(CH_3CN)](BF_4)_3$ (**8c**) exhibit significant catalytic activity for CO_2 reduction. Controlled-potential electrolysis of **8a** indicated a current efficiency for CO production of approximately 15% under conditions similar to those described for **8c**. The cyclic voltammetry data for **8a** are also very similar to those described for **8c**. It is interesting that no CO_2 reduction was observed for the nickel−acetonitrile complex, $[Ni(Bu_3P^+etpE)(CH_3CN)](BF_4)_3$ (**8b**), or for the palladium−acetonitrile complex with terminal phosphonium substituents, $[Pd(etpPBu_3^+)(CH_3CN)](BF_4)_6$ (**9**).

The catalytic current can be used to obtain kinetic information on the catalytic process. The dependence of the catalytic current on the concentration of **8c** and on CO_2 concentration is shown in Figure 7. The linear dependence of the catalytic current on the catalyst concentration is consistent with a rate-determining step that is first order in catalyst.[24] Similarly, the linear dependence of the catalytic current on the square root of the CO_2 concentration implies a rate-determining step at high acid concentrations that is first order in CO_2. The observation that the rate-determining step at high acid concentrations is first order in CO_2 and first order in catalyst provides additional evidence for the second step of eq 4. The deviation from linearity at higher catalyst concentrations, which is observed in the bottom graph of Figure 7, is likely due to catalyst decomposition to the Pd(I) dimer **13** shown in the last step of eq 4. The results obtained for the catalyst under noncatalytic and catalytic conditions are internally consistent and support the mechanistic steps shown in eq 4.

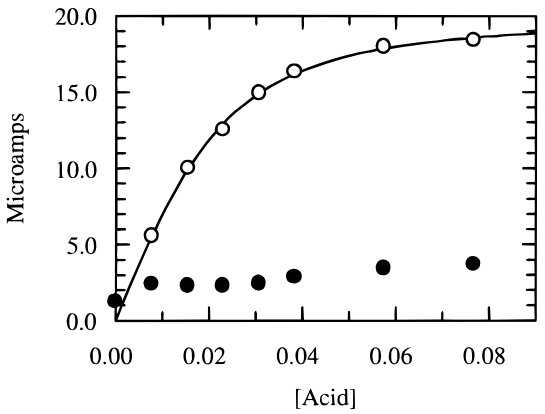

Figure 8. Dependence of the peak current on the concentration of HBF_4 for dimethylformamide solutions containing 0.0013 M $[Pd(Me_3P^+etpE)(CH_3CN)](BF_4)_3$ (**8c**) and 0.18 M CO_2 (○). Dependence of the peak current on the concentration of HBF_4 for dimethylformamide solutions containing 0.0013 M $[Pd(Me_3P^+etpE)(CH_3CN)](BF_4)_3$ under nitrogen (●). The solid line shows the best-fit line using eq 5 with $k_1 = 310$ and $k_2 = 8.2 \times 10^4$.

The current dependence on acid concentration is biphasic, as shown in Figure 8. This biphasic character implies the existence of two rate-determining steps. At low acid concentrations, the current exhibits a first-order dependence on acid, which indicates a transition state involving two protons. At higher acid concentrations, the current is independent of the acid concentration. Equation 5 can be used to fit the dependence of the catalytic current on acid, CO_2, and catalyst concentrations.[9,25] In eq 5, n is the number of electrons

$$\frac{i_c}{i_d} = \frac{\sigma}{0.447}\sqrt{\frac{RT}{nF\nu}}\sqrt{\frac{k_1 k_2 [CO_2][H^+]^2}{k_1[CO_2] + k_2[H^+]^2}} \qquad (5)$$

involved in catalyst reduction, ν is the scan rate, σ is a factor that depends on whether the second electron is transferred at the electrode or in solution,[25] k_1 is the second-order rate constant for the reaction of CO_2 with the reduced catalyst, and k_2 is a third-order rate constant that undoubtedly is not a simple rate constant. On the basis of the curve fit shown in Figure 8, the second-order rate constant for the reaction of CO_2 with the Pd(I) intermediate **11** is calculated to be 310 M^{-1} s^{-1} for $[Pd(Me_3P^+etpE)(CH_3CN)](BF_4)_3$ (**8c**), assuming a value of 2 for σ.[26] For $[Pd(Bu_3P^+etpE)(CH_3CN)](BF_4)_3$ (**8a**), a value of 450 M^{-1} s^{-1} was obtained.

(24) Savéant, J.-M.; Vianello, E. *Electrochim. Acta* **1965**, *10*, 905. Hammouche, M.; Lexa, D.; Momenteau, M.; Savéant, J.-M. *J. Am. Chem. Soc.* **1991**, *113*, 8455.

(25) Savéant, J.-M.; Su, K. B. *J. Electroanal. Chem.* **1985**, *196*, 1.

(26) In previous work we have assumed a value of 2 for σ as well. This value implies that the second electron transfer occurs at the electrode surface and not in solution. The rate constant calculated using 2 is one-half the rate obtained if the square root of 2 is used, which would be correct for an electron-transfer process occuring exclusively in solution. A detailed discussion of the differences between catalytic processes in which the second electron transfer occurs in solution or at the electrode surface can be found in refs 24 and 25. The use of a value of 2 for σ results in a conservative estimate of the rate constant as well as one that is consistent with earlier studies.

The CO_2 intermediate, **12**, can decompose to dimer **13** or be protonated to ultimately form **14**. The precise sequence of steps leading from **12** to **14** is not known, but there is evidence for steps involving protonation of **12**, a second electron transfer, and solvent loss. The second-order dependence of the rate-determining step on acid at low acid concentrations is consistent with protonating complex **12** in two steps. We believe a second electron transfer step follows protonation of **12** for the following reasons. (1) In the absence of acid, no second electron transfer occurs at the potential of the first reduction wave (Figure 5, solid circles). In the presence of acid, this wave increases dramatically (Figure 6, dashed Line). On the basis of these observations, a protonation step precedes the second electron transfer. (2) In previous work, we have shown that analogous palladium catalysts containing triphosphine ligands with two trimethylene linkages between the phosphorus atoms (as opposed to two ethylene linkages in **8a** and **8c**) exhibit a first-order dependence on acid consistent with only one proton in the transition state.[11] This result implies that a second protonation is not required for a second electron transfer in this closely related system. For these reasons, it seems likely that the second electron transfer occurs after the first protonation of **12** but before the second protonation.

In converting **12** to **14**, solvent loss is required in addition to the protonation and electron-transfer steps. Solvent loss is thought to occur during the catalytic cycle for two reasons. First, replacing acetonitrile with strongly coordinating ligands such as phosphines quenches the catalytic reaction, even though these $[Pd(triphosphine)(PR_3)](BF_4)_2$ complexes will react with CO_2 upon reduction.[9] For example, $[Pd(Bu_3P^+etpE)(PEt_3)](BF_4)_2$ (**10**) is not catalytically active in DMF solutions. Second, strongly coordinating solvents such as dimethyl sulfoxide also inhibit the catalytic reaction. Complex **8c** does not exhibit a catalytic wave in the presence of CO_2 and acid when dimethyl sulfoxide is used as a solvent. However, because the peak current is decreased and the peak potential is shifted in a positive direction when CO_2 is added to nonacidic dimethyl sulfoxide solutions, **8c** appears to react rapidly with CO_2 following a one-electron reduction. Consequently, the decrease in catalytic activity observed in acidic dimethyl sulfoxide is not caused by inhibition of the reaction of the catalyst with CO_2. This is consistent with CO_2 reacting with the Pd(I) species, **11**, before solvent loss, as discussed above. Whether solvent loss occurs immediately after formation of **12** or following the protonation or electron-transfer steps preceding formation of **14** is not clear.

Protonation of **14** to form **15** followed by a rate-determining cleavage of a C-O bond is consistent with the observed second-order dependence on acid, eq 6. Similar reactions have been reported for $[Pt(PEt_3)_2(C_6H_5)(COOH)]$[27] and $[Pt(PEt_3)_2(Cl)(COOMe)]$.[28] These complexes undergo protonation to form carbonyl complexes analogous to **16** and water or methanol, respectively. The apparent requirement for solvent loss prior to C−O bond cleavage is interesting and suggests that the presence of a vacant coordination site may be important in assisting C−O bond cleavage to form **16**. The carbonyl complex **16** has not been detected spectroscopically when complexes **8a** and **8c** are dissolved in weakly coordinating solvents such as dichloromethane under a CO atmosphere, but we believe it is a likely intermediate since the product of the catalytic reaction is CO. The observation that **16** is not formed from **8a** or **8c** is consistent with catalytic formation of CO. If **16** were stable, the catalytic rate would be inhibited by CO but this is not observed.

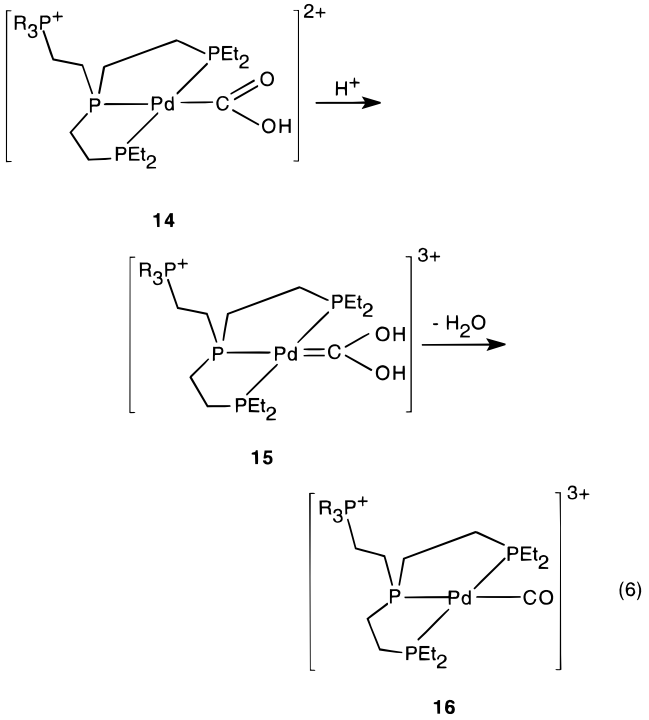

(6)

Discussion

The rate of CO_2 reduction for the bimetallic complex **2** is enhanced by at least 3 orders of magnitude compared to monomeric complexes of type **1**.[12] This enhancement has been attributed to the cooperative binding of CO_2 in which one palladium atom is bound to carbon and a second palladium atom is bound to oxygen. Structural studies have confirmed MC(O)OM′ linkages for complexes in which M is a transition metal and M′ is a transition metal, a main group metal, or an alkali metal.[29] It has also been recently demonstrated that the sulfonate groups used for generating water-soluble catalysts can have significant effects on catalytic reactions.[30] It was, therefore, of interest to see if positively charged phosphonium groups attached to either the central or terminal phosphorus atoms of the triphosphine ligand of monomeric palladium complexes, such as **1**, would produce significant changes in the catalytic rates or mechanisms. For such complexes, the formation of catalytic intermediates, such as **12**, might be facilitated by stabilizing the negative charge that develops on CO_2 by interaction with the positively charged phosphonium group.

Although the base-catalyzed reaction of secondary phosphines with vinylphosphonium salts has been

(27) Bennet, M. A.; Robertson, G. B.; Rokicki, A.; Wickramasinghe, W. A. *J. Am. Chem. Soc.* **1988**, *110*, 7098.
(28) Byrd, J. E.; Halpern, J. *J. Am. Chem. Soc.* **1971**, *93*, 1634.
(29) For a comprehensive review of the bonding in CO_2 complexes, see: Gibson, D. H. *Chem. Rev.* **1996**, *96*, 2063.
(30) Buriak, J. M.; Osborn, J. A. *Organometallics* **1996**, *15*, 3161.

reported, we found that extension of this reaction to triphosphine ligands **3** and **6** led to intractable mixtures of products. This prevented the direct synthesis of triphosphine ligands such as **4**. The formation of tributylphosphine in reaction 1 indicated that a nucleophilic attack of the diethylphosphino groups of **3** on the vinyl group might be occurring with subsequent transfer of the vinyl cation from the vinyltributylphosphonium cation. This suggested that if the lone pairs of the triphosphine ligand could be rendered inaccessible by coordination to a metal, then the P−H addition to the vinylphosphonium salt might proceed cleanly. This was found to be the case, as the synthesis of the bromide complexes **5a**, **5b**, **7a**, and **7b** are readily carried out in one-pot reactions, as shown in eqs 2 and 3. The sequence of addition of the reagents in these one-pot reactions is important if insoluble precipitates attributed to phosphido-bridged species are to be avoided. The bromide complexes can be converted to the corresponding acetonitrile complexes **8a**−**c** and **9** by reaction with silver tetrafluoroborate in acetonitrile. In previous studies, weakly solvated acetonitrile complexes have proven to be the best catalysts.[9]

The structural studies of [Ni(etpPBu$_3^+$)Br]Br(BF$_4$)$_4$ (**7b**) and [Pd(Bu$_3$P$^+$etpE)(CH$_3$CN)](BF$_4$)$_3$ (**8a**) verified the addition of the P−H bonds to the vinylphosphonium cations. In addition, the presence of a bromide ion in a pocket formed by two tributylphosphonium substituents in **7b** and the close association of a BF$_4^-$ anion with a palladium atom and a phosphonium group in **8a** are both indicative of the ability of the phosphonium groups to interact with negatively charged species.

Kinetic studies of [Pd(Bu$_3$P$^+$etpE)(CH$_3$CN)](BF$_4$)$_3$ and [Pd(Me$_3$P$^+$etpE)(CH$_3$CN)](BF$_4$)$_3$ were carried out to determine if the mechanism for electrocatalytic reduction of CO_2 to CO was altered by the presence of the phosphonium substituents and if the catalytic rate was enhanced or decreased compared to complexes without phosphonium substituents. Similar studies were not possible for [Pd(etpPBu$_3^+$)(CH$_3$CN)](BF$_4$)$_6$ (**9**), which contained four terminal phosphonium substituents, because no catalytic current was observed for CO_2 reduction. Complexes **8a** and **8c** both exhibit a biphasic dependence on acid, consistent with two rate-determining steps (Figure 8). At high acid concentrations, there is no acid dependence and the rate-determining step is first order in CO_2 and first order in complex (Figure 7). This suggests the reaction of a Pd(I) intermediate with CO_2 as the rate-determining step, as shown in eq 4. At low acid concentrations, a second-order dependence on acid is observed. This is consistent with a rate-determining step that involves either a slow second protonation or cleavage of the carbon−oxygen bond (as shown in eq 6) to form coordinated CO and water. These mechanistic features are the same as those observed previously for other [Pd(triphosphine)(solvent)](BF$_4$)$_2$ complexes with two carbon chains between the three phosphorus atoms. On this basis, the phosphonium groups do not appear to significantly alter the reaction mechanism.

The rate constants observed for **8a** (450 M^{-1} s^{-1}) and **8c** (310 M^{-1} s^{-1}) for the reaction of the reduced catalyst with CO_2 are both approximately 30−50% higher than the rates expected on the basis of their respective redox potentials, −1.52 and −1.45 V.[10] These values indicate that there is no significant enhancement of the rate produced by the presence of a pendant phosphonium group on the central phosphorus atom. On the other hand, no significant decrease in the rate is observed either. These results suggest that the noncoordinating phosphonium groups may be useful in introducing water solubility without significantly affecting catalytic rates or mechanisms.

Summary

Synthetic procedures have been developed for incorporating phosphonium substituents on nickel and palladium complexes containing triphosphine ligands. Studies of the catalytic mechanisms and rates for [Pd(Bu$_3$P$^+$etpE)(CH$_3$CN)](BF$_4$)$_3$ (**8a**) and [Pd(Me$_3$P$^+$etpE)(CH$_3$CN)](BF$_4$)$_3$ (**8c**) indicate that phosphonium substituents do not significantly alter the mechanism or rates of CO_2 reduction by these complexes compared to complexes without these substituents. The incorporation of a second metal, as shown in structure **2**, appears to be much more effective in enhancing catalytic rates. The role of pendant phosphonium groups for immobilizing catalysts in cation-exchange membranes attached to electrode surfaces is under investigation.

Experimental Section

General Comments. All reactions were carried out under a nitrogen atmosphere using standard Schlenk techniques. Dichloromethane and acetonitrile were distilled from calcium hydride under nitrogen. Dimethylformamide (Burdick and Jackson) was stored under nitrogen. ^{1}H and ^{31}P NMR spectra were recorded on a Varian Unity 300 MHz spectrometer at 299.75 and 121.42 MHz, respectively. ^{1}H chemical shifts are reported relative to tetramethylsilane using residual solvent protons as a secondary reference. ^{31}P chemical shifts are reported relative to external phosphoric acid. Elemental analyses were performed by Schwarzkopf Microanalytical Laboratory, Inc. [Ni(NCCH$_3$)$_6$](BF$_4$)$_2$,[31] [Pd(NCCH$_3$)$_4$](BF$_4$)$_2$,[32] vinyltributylphosphonium bromide,[14] bis(2-(diethylphosphino)-ethyl)phosphine (HetpE, **3**),[8] and bis(2-phosphinoethyl)phenylphosphine (etpH, **6**)[8] were prepared according to literature methods.

Coulometric measurements were carried out at 21−25 °C using a Cypress Systems CS-2000 computer-controlled potentiostat/galvanostat. The working electrode was constructed from a reticulated vitreous carbon rod with a diameter of 1 cm and length of 2.5 cm (60 pores per in., The Electrosynthesis Co., Inc.), the counter electrode was a Pt wire, and a Ag wire immersed in a permethylferrocene/permethylferrocenium solution was used as the pseudoreference electrode.[31] The electrode compartments were separated by Vycor disks (7-mm diameter, EG&G Princeton Applied Research).

Catalytic coulometric experiments were carried out in a sealed flask (148 mL volume) from which aliquots were removed for GC analysis. Turnover numbers were determined by measuring the amount of CO produced when the catalytic current had decayed to 5−10% of its original value in the presence of 0.18 M CO_2 and 0.1 M HBF$_4$ (i.e., the same as the initial conditions). Analyses of the gases produced were carried out using a 100/120 Carbosieve S-II stainless steel column with dimensions 10 ft × 1/8 in. from Supelco: 200 °C; flow rate, 30 mL/m; Ar carrier gas. Calibration curves were constructed by adding known amounts of CO and hydrogen to the reaction flask containing solvent and supporting elec-

(31) Hathaway, B. J.; Holah, D. G.; Underhill, A. E. *J. Chem. Soc.* **1962**, 2444.
(32) Sen, A.; Ta-Wang, L. *J. Am. Chem. Soc.* **1981**, *103*, 4627.
(33) Bashkin, J. K.; Kinlen, P. *Inorg. Chem.* **1990**, *29*, 4507.

trolyte. These curves were used to determine yields of CO and hydrogen produced during catalytic runs. Current efficiencies for CO and H_2 production were calculated using these yields and the total charge passed during the electrolysis experiment. Cyclic voltammetry and chronoamperometry experiments were carried out using a Cypress Systems CS-1190 computer-controlled electroanalytical system at 21 ± 1 °C unless stated otherwise. The working electrode was a glassy carbon electrode (Cypress Systems, Inc.). Ferrocene was used as an internal standard, and all potentials are reported vs the ferrocene/ferrocenium couple.[34] The solubility of CO_2 in dimethylformamide was taken from ref 35. All solutions for CV and coulometric experiments were 0.3 N NEt_4BF_4 in dimethylformamide.

Syntheses. [Pd(Bu$_3$P$^+$etpE)(Br)](BF$_4$)$_2$, 5a. A solution of HetpE (0.27 g, 1.0 mmol) in acetonitrile (20 mL) was added to a mixture of $[Pd(CH_3CN)_4](BF_4)_2$ (0.44 g, 1.0 mmol) and vinyltributylphosphonium bromide (0.32 g, 1.0 mmol) in acetonitrile (20 mL). The reaction mixture was stirred at room temperature for 1 h, then triethylamine (0.25 mL) was added via syringe. The resulting solution was heated to 80 °C and stirred for 1 h. The solvent was removed in a vacuum to produce a yellow oil. White crystals (0.39 g, 46%) were obtained by dissolving the oil in hot ethanol and cooling the resulting solution to room temperature. Anal. Calcd for $C_{26}H_{59}B_2BrF_8PdP_4$: C, 36.5; H, 7.0; Br, 9.2; P, 14.5. Found: C, 36.2; H, 6.8; Br, 9.2; P, 13.6.

[Pd(Bu$_3$P$^+$etpE)(CH$_3$CN)](BF$_4$)$_3$, 8a. The yellow oil obtained using the procedure described in the preceding paragraph was dissolved in acetonitrile (30 mL). Addition of $AgBF_4$ (0.19 g) to this solution produced a brown precipitate. After the reaction mixture was stirred for an additional 0.5 h, it was filtered and the solvent was removed from the filtrate by applying a vacuum to produce a brown solid. This solid was washed with ethyl acetate (2 10-mL portions) and dissolved in dichloromethane (10 mL). The resulting solution was filtered again to remove residual AgBr. Acetonitrile (1 mL) and methanol (10 mL) were added to the filtrate, and the volume was reduced to approximately 5 mL in a vacuum. After the flask was placed in a refrigerator overnight, a tan microcrystalline product was obtained. The solid was collected by filtration and washed with ether to obtain an off-white powder (0.51 g, 56%). Anal. Calcd for $C_{28}H_{62}NB_3F_{12}P_4Pd$: C, 37.2; H, 6.9; N, 1.6. Found: C, 36.7; H, 6.8; N, 1.8. X-ray quality crystals were grown from a solution of ethyl acetate and metylene chloride containing approximately 5% acetonitrile. IR (Nujol mull): ν(CN) 2300 and 2328 cm^{-1}.

[Pd(Bu$_3$P$^+$etpE)(PEt$_3$)](BF$_4$)$_3$, 10. Triethylphosphine (0.1 g, 0.85 mmol) was added to a solution of $[Pd(Bu_3P^+etpE)(CH_3CN)](BF_4)_3$ (0.20 g, 0.22 mmol) in acetone. The reaction mixture was stirred at room temperature for 0.5 h, then the solvent was removed by applying a vacuum. The resulting yellow solid (0.21 g, 97%) was washed with ether and dried in a vacuum. Anal. Calcd for $C_{32}H_{74}B_3F_{12}PdP_5$: C, 39.2; H, 7.6; P, 15.8. Found: C, 39.0; H, 7.5; P, 13.5.

[Pd(Me$_3$P$^+$etpE)(CH$_3$CN)](BF$_4$)$_3$, 8c. This compound was prepared in a manner analogous to $[Pd(Bu_3P^+etpE)(CH_3CN)](BF_4)_3$ using vinyltrimethylphosphonium bromide rather than vinyltributylphosphonium bromide. Anal. Calcd for $C_{19}H_{44}B_3F_{12}NPdP_4$: C, 29.4; H, 5.7; N, 1.8. Found: C, 29.3; H, 5.4; N, 1.8. IR (Nujol mull): ν(CN) 2296 and 2325 cm^{-1}.

[Ni(Bu$_3$P$^+$etpE)(Br)](BF$_4$)$_2$, 5b. A solution of HetpE (0.27 g, 1.0 mmol) in acetonitrile (20 mL) was added to a mixture of $[Ni(CH_3CN)_6](BF_4)_2 \cdot 0.5CH_3CN$ (0.50 g, 1.0 mmol) and vinyltriethylphosphonium bromide (0.32 g, 1.0 mmol) in acetonitrile (20 mL). The reaction mixture was stirred at room temperature for 1 h, then triethylamine (0.25 mL) was added via syringe. The resulting solution was stirred for 1 h at room temperature, and the solvent was removed in a vacuum to produce a red solid. Orange crystals (0.30 g, 37%) were obtained by dissolving the solid in hot ethanol and cooling to room temperature. Anal. Calcd for $C_{26}H_{59}B_2BrF_8NiP_4$: C, 36.5; H, 7.0; Br, 9.2; P, 14.5. Found: C, 36.2; H, 6.8; Br, 9.2; P, 13.6.

[Ni(Bu$_3$P$^+$etpE)(CH$_3$CN)](BF$_4$)$_3$, 8b. A solution of HetpE (0.27 g, 1.0 mmol) in acetonitrile (20 mL) was added to a mixture of $[Ni(CH_3CN)_6](BF_4)_2 \cdot 0.5CH_3CN$ (0.50 g, 1.0 mmol) and vinyltriethylphosphonium bromide (0.32 g, 1.0 mmol) in acetonitrile (20 mL). The red-brown reaction mixture was stirred at room temperature for 1 h, then triethylamine (0.25 mL) was added via syringe. After an additional hour, a solution of $AgBF_4$ in acetonitrile (20 mL) was added. A white precipitate formed immediately. The fine precipitate was separated from the solution by placing the reaction mixture in a centrifuge operating at 2000 rpm for 30 min. The volume of the solution obtained by decanting the reaction mixture was reduced to approximately 10 mL, and diethyl ether was added to produce a tan solid. This solid (0.24 g, 28%) was collected by filtration and dried in a vacuum. Anal. Calcd for $C_{28}H_{62}NB_3F_{12}P_4Ni$: C, 39.3; H, 7.3; N, 1.6. Found: C, 36.5; H, 7.1; N, 1.5. IR (Nujol mull): ν(CN) 2299 and 2329 cm^{-1}.

[Pd(etpPBu$_3^+$)(Br)]Br(BF$_4$)$_4$, 7a. A solution of etpH (0.23 g, 1.0 mmol) in acetonitrile (5 mL) was added to a red solution of $[Pd(CH_3CN)_4](BF_4)_2$ (0.44 g, 1.0 mmol) and vinyltributylphosphonium bromide (1.29 g, 4.0 mmol) in acetonitrile (25 mL) to produce a yellow precipitate. The reaction mixture was stirred at room temperature for 1 h, then triethylamine (0.25 mL) was added via syringe. The heterogeneous mixture was heated to 80 °C overnight to produce a dark solution. The solvent was removed in a vacuum to produce a red oil. The oil was dissolved in dichloromethane (50 mL) and extracted with water (3 30-mL aliquots). A brown solid formed when the solvent was removed with a vacuum. This product was dissolved in acetonitrile (2 mL), and ethyl acetate (20 mL) was added to the resulting solution. Cooling the solution in a freezer overnight resulted in the formation of tan crystals (0.51 g, 29%), which were collected by filtration and dried in a vacuum. Anal. Calcd for $C_{66}H_{137}B_4Br_2F_{16}PdP_7$: C, 45.0; H, 7.8; Br, 9.1. Found: C, 44.5; H, 8.0; Br, 8.9.

[Pd(etpPBu$_3^+$)(CH$_3$CN)](BF$_4$)$_6$, 9. Solid $AgBF_4$ (0.79 g, 4.0 mmol) was added to a solution of crude $[Pd(etpP^+Bu_3)(Br)]Br(BF_4)_4$ (1.0 mmol, obtained as described in the preceding paragraph but without recrystallization) in acetonitrile (50 mL), and the resulting reaction mixture was stirred overnight at room temperature. AgBr was removed by filtration, and the solvent was removed from the filtrate with a vacuum to produce an orange oil. The oil was dissolved in dichloromethane (20 mL) and washed with water (3 20-mL aliquots). Removal of the solvent with a vacuum produced a brown solid (1.20 g). We were unable to obtain satisfactory analytical data for this complex after repeated attempts to recrystallize the product. The major impurity is unreacted vinyltributylphosphonium salt, which could be observed by ^{31}P NMR.

[Ni(etpPBu$_3^+$)(Br)]Br(BF$_4$)$_4$, 7b. This compound was prepared as described for the analogous Pd complex. X-ray quality crystals were grown by slow evaporation in air of a 1:2 dichloromethane/ethyl acetate mixture.

Electrochemical Reduction of 8a under CO$_2$. $[Pd(Bu_3P^+etpE)(CH_3CN)](BF_4)_3$ (0.038 g, 0.042 mmol) was dissolved in a DMF solution containing 0.3 M NEt_4BF_4 and saturated with CO_2. This solution was electrolyzed at −1.65 V, which resulted in the passage of 4.01 C of charge. The ^{31}P NMR spectrum of the reduction product, **13**, is consistent with an ABMX system. ^{31}P NMR: P_C (the central phosphorus atom of the tridentate ligand), 64.45 ppm (*61.1 ppm*) (dd, $J_{P_C-PEt_2}$ = 345 Hz (*350 Hz*), $J_{P_C-P^+}$ = 29 Hz); Et_2P (trans to Pd), 46.05 ppm (*40.9 ppm*) (s); Bu_3P^+, 35.76 ppm (d); PEt_2 (trans to P), 23.80 ppm (*23.3 ppm*) (d). The values in italics are for the analogous $[Pd(etpE)]_2(BF_4)_2$ complex which has been characterized crystallographi-

(34) Gagne, R. R.; Koval, C. A.; Lisensky, G. C. *Inorg. Chem.* **1980**, *19*, 2855. Gritzner, G.; Kuta, J. *Pure Appl. Chem.* **1984**, *56*, 461. Hupp, J. T. *Inorg. Chem.* **1990**, *29*, 5010.

(35) *Solubilities of Inorganic and Organic Compounds*; Stephen, H., Stephen, T., Eds.; Pergamon: New York, 1958; Vol. 1, p 1063.

Table 5. Crystal Data, Data Collection Parameters, and Solution Refinement Details for [Ni(etpPBu$_3^+$)Br](BF$_4$)$_4$Br (7b) and [Pd(Bu$_3$P$^+$etpE)(CH$_3$CN)](BF$_4$)$_3$ (8a)

	7b	8b
	Crystal Data	
empirical formula	$C_{71}H_{147}B_{3.89}Br_{2.11}Cl_2F_{15.55}NiO_2P_7$	$C_{28}H_{62}B_3F_{12}NP_4Pd$
fw	1885.62	903.50
cryst size, mm	0.50 × 0.42 × 0.42	0.13 × 0.62 × 0.64
cryst color, habit	orange parallelepiped	colorless thin plate
cryst system	monoclinic	monoclinic
space group	$P2_1/n$	$P2_1$
a, Å	13.7410(2)	14.5165(2)
b, Å	26.4174(4)	13.57180(10)
c, Å	27.0923(4)	21.2465(2)
α, deg	90	90
β, deg	103.25	95.9480(10)
γ, deg	90	90
volume, Å^3	9572.7(2)	4163.34(8)
Z, formula units/cell	4	4
density (calculated), g·m^{-3}	1.308	1.441
abs coeff, mm^{-1}	1.325	0.674
F(000)	3957	1864
abs corr	semiempirical	semiemperical
transmission coeff	0.52 and 0.63	0.701 and 0.934
	Data Collection	
diffractometer	Siemens SMART CCD	Siemens SMART CCD
temperature, K	167(2)	162(2)
radiation source	sealed tube	sealed tube
wavelength, Å	0.710 73 Mo Kα	0.710 73 Mo Kα
monochromator	graphite	graphite
cell measurement		
no. of reflns used	8192	8192
θ range	1.09 < *θ* < 25.00	0.96 < *θ* < 28.29
θ range, data collection, deg	1.09 < *θ* < 25.00	0.96 < *θ* < 27.50
scan type	*ω* scans	*ω* scans
index ranges	$-17 \le h \le 17$, $-34 \le k \le 34$, $-30 \le l \le 35$	$-19 \le h \le 19$, $-18 \le k \le 14$, $-28 \le l \le 25$
no. of reflns collected	51 511	27 370
no. of indep reflns	16 840 (R(int) = 0.0445)	15 999 (R(int) = 0.0211)
no. of standard reflns	50 frames remeasured	50 frames remeasured
stability of standards	no decay observed	no decay observed
	Structure Solution and Refinement	
system used[a]	Siemens SHELXTL	Siemens SHELXTL
structure solution	direct	direct
data/restraints/params	16738/78/993	15986/1/885
hydrogen atoms	riding with riding isotropic U	riding with riding isotropic U
weighting scheme	calcd $w^{-1} = [\sigma^2(F_o^2) + (0.0713P)^2 + 45.0065P]$, where $P = (F_o^2 + 2F_c^2)/3$	calcd $w^{-1} = [\sigma^2(F_o^2) + (0.0527P)^2 + 4.5125P]$, where $P = (F_o^2 + 2F_c^2)/3$
final R indices[b] [$I > 2\sigma(I)$]	R1 = 0.0718, wR2 = 0.1796	R1 = 0.0422, wR2 = 0.1023
no. of reflns observed	13 010	14 173
R indices (all data)	R1 = 0.0962, wR2 = 0.1973	R1 = 0.0513, wR2 = 0.1118
goodness-of-fit[c] on F^2	1.121	1.037
largest diff peak and hole	1.946 and −0.771	0.964 and −0.851

[a] Reference 36 [b] R1 = $[\sum||F_o| - |F_c||]/[\sum|F_o|]$; wR2 = $([\sum[w(F_o^2 - F_c^2)^2]]/[\sum[w(F_o^2)^2]])^{1/2}$. [c] GooF = $S = ([\sum[w(F_o^2 - F_c^2)^2]]/(M - N))^{1/2}$, where M is the number of reflections and N is the number of parameters refined.

cally.[9] A cyclic voltammogram of the reduction product exhibited an irreversible cathodic wave at −2.00 V (*−1.86 V)* and an irreversible anodic wave at +0.72 V (*+0.58 V)*.

Reaction of HetpE, 3, with Vinyltributylphosphonium Bromide. Vinyltributylphosphonium bromide (0.060 g, 0.2 mmol) was added to an NMR tube containing HetpE (0.012 g, 0.05 mmol) and a trace amount of KO^{t}Bu in acetonitrile. After 0.5 h, resonances were observed in the ^{31}P NMR consistent with the desired product [(Bu$_3$PCH$_2$CH$_2$)P(CH$_2$CH$_2$PEt$_2$)$_2$]Br. ^{31}P NMR (CH$_3$CN): Bu$_3$P$^+$, 36.4 ppm (d, $^3J_{PP}$ = 32 Hz); P$_C$, −15.0 ppm (dt, $^3J_{PP}$ = 22 Hz); PEt$_2$, −17.6 (d). In addition, resonances were also observed for PBu$_3$ (−31 ppm) and numerous other products. A similar reaction between vinyltributylphosphonium bromide and triethylphosphine (no base) also produced a resonance at −31 ppm assigned to tributylphosphine.

X-ray Diffraction Studies. Crystal data, data collection parameters, and solution refinement details for **7b** and **8a** are given in Table 5. Data collections were performed using a Siemens SMART diffractometer consisting of a two-dimensional CCD detector mounted on a PLATFORM three-circle goniometer equipped with an LT-2A low-temperature apparatus and a K760 X-ray generator. Cell parameters were determined after indexing reflections harvested from three orthogonal sets of 20 scans and were refined using reflections with $I > 10\sigma(I)$ harvested from the data collection. The data collection employed 0.3° *ω* scans, each frame was comprised of two 15-sec scans correlated to reduce noise and errors. The first 50 frames were remeasured on completion of the data collection. No decay was observed in either study. In each experiment, more than a hemisphere of data was collected. Redundant reflections were merged. All data were corrected for Lorentz and polarization effects as well as for absorption. Structure solution and refinement, as well as molecular graphics, utilized the SHELXTL[36] suite of programs installed on a Silicon Graphics Indigo2 workstation. Neutral atom

(36) Seldrick, G. M. *SHELXTL, A Program for Crystal Structure Determination*, Version 5.03; Siemens Analytical X-ray Instruments: Madison, WI, 1995.

scattering factors were from a standard source.[37] Full details of the structure determinations are available as supporting information.

Acknowledgment. This work was supported by the U.S. Department of Energy, Office of Basic Energy Sciences, Chemical Sciences Division.

(37) Scattering factors (neutral atoms) are from *International Tables for Crystallography*; Reidel Publishing Co.: Boston, MA, 1991; Vols. C, D.

Supporting Information Available: Tables of crystal data, data collection conditions, solution and refinement details, atomic coordinates and equivalent isotropic displacement parameters, bond lengths, bond angles, anisotropic displacement parameters, and hydrogen atom coordinates and isotropic parameters of **7b** (Tables 1s−8s) and **8a** (Tables 9s−16s) (38 pages). Ordering information is given on any current masthead page.

OM970519C